

A probabilistic approach for the evaluation of the stabilizing forces of fully grouted bolts

Original

A probabilistic approach for the evaluation of the stabilizing forces of fully grouted bolts / Oreste, P., Spagnoli, G.. - In: TRANSPORTATION GEOTECHNICS. - ISSN 2214-3912. - STAMPA. - 28:(2021), p. 100516.
[10.1016/j.trgeo.2021.100516]

Availability:

This version is available at: 11583/2941014 since: 2021-11-28T21:12:27Z

Publisher:

Elsevier Ltd

Published

DOI:10.1016/j.trgeo.2021.100516

Terms of use:

This article is made available under terms and conditions as specified in the corresponding bibliographic description in the repository

Publisher copyright

(Article begins on next page)

24 the safety factors of the rock block, one for each diameter of the steel bars used for its
25 stabilization. Finally, the probabilistic management of the safety factor samples
26 allowed the correct design of the steel bars, by evaluating the probability that the safety
27 factor of the block with regard to potential slipping has a value lower than a pre-
28 established limit. The probabilistic approach developed was applied to a real problem
29 of stabilization of a potentially unstable rock block due to planar sliding, present on a
30 municipal road in North Italy.

31 **Keywords:** rock bolt; Winkler spring approach; rock block stabilisation; safety factor;
32 Monte Carlo simulation, probabilistic approach,

33

34 **Abbreviations and nomenclature**

| | | |
|----|----------------------|----------------------------------------------------------------------------|
| 35 | A | Area of the sliding surface of the block; |
| 36 | A_{bar} | Area of the section of the steel bar constituting the bolt |
| 37 | c | Cohesion on the natural discontinuity which constitutes the sliding |
| 38 | | surface; |
| 39 | $(EA)_{bolt}$ | Axial stiffness of the bolt |
| 40 | E_{binder} | Elastic modulus of the binder surrounding the steel bar in the hole |
| 41 | $(EJ)_{bolt}$ | Bending stiffness of the bolt |
| 42 | E_{st} | Steel elastic modulus |
| 43 | $f(x)$ | Probability density associated with the x value of the geotechnical or |
| 44 | | geomechanical parameter considered; |
| 45 | F_S | Safety factor; |
| 46 | J_{bar} | Moment of inertia of the steel bar constituting the bolt |
| 47 | k | Ratio between the normal pressure, p , which is applied on the perimeter |
| 48 | | of the bolt (on the wall of the hole) by the surrounding rock and the |
| 49 | | normal displacements, y , of the bolt |
| 50 | L_a | Bolt length inside the unstable block |
| 51 | L_p | Bolt length in the stable rock behind the unstable block |
| 52 | L_{test} | Length of the tested bolt |
| 53 | M | Bending moment in the bolt |
| 54 | N | Axial force in the bolt |
| 55 | $N_{0,\delta_{max}}$ | Bolt stabilising force in the direction of the bolt axis |
| 56 | N_{test} | Tensile axial force applied at the bolt head from pull-out tests |
| 57 | N_{yield} | Force causing the bar failure under tensile stress |
| 58 | N_{slip} | Force causing the bolt-rock interface to fail for a unit bolt length |

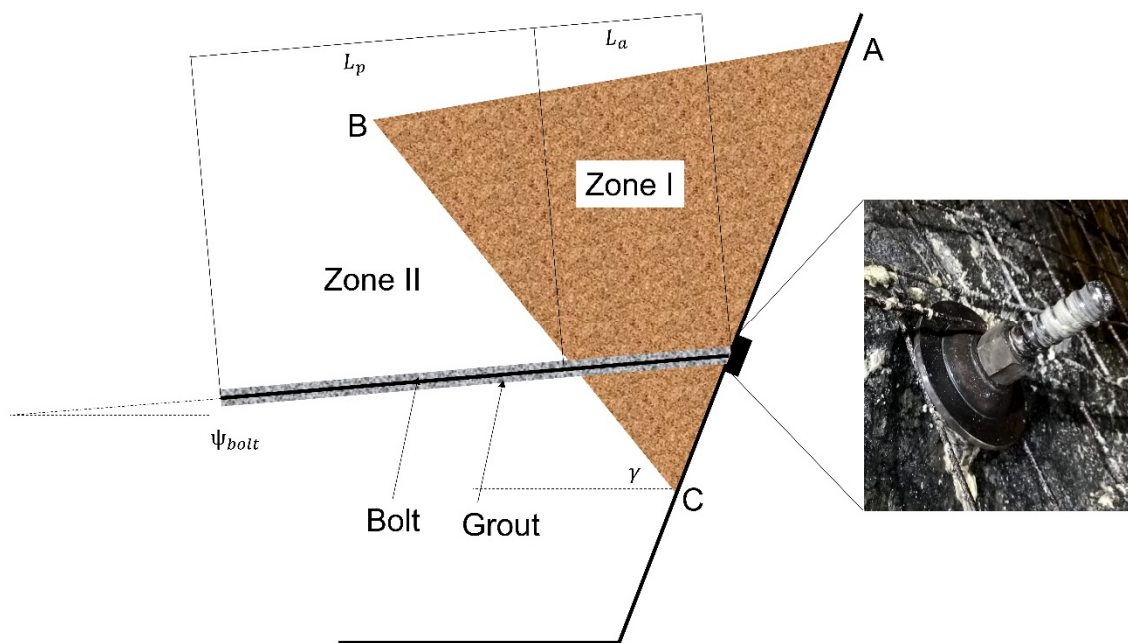
| | | |
|----|----------------------|------------------------------------------------------------------------------------------------------|
| 59 | N_0 | Value of the tensile force in the axial direction of the bolt on the |
| 60 | | intersection point between the bolt and a block surface |
| 61 | n | Number of fully grouted passive bolts present; |
| 62 | T | Shear force in the bolt |
| 63 | t_{binder} | Thickness of the binder annulus surrounding the steel bar |
| 64 | T_0 | Value of the shear force perpendicular to the axial direction of the bolt |
| 65 | | on the intersection point between the bolt and a block surface |
| 66 | $T_{0,\delta_{max}}$ | Bolt stabilising force in the transverse direction |
| 67 | v_r | Value of the relative axial displacement between the bolt and the |
| 68 | | surrounding rock |
| 69 | W | Weight of the potentially unstable rock block; |
| 70 | y | Normal displacements of the bolt perpendicular to the axial direction of |
| 71 | | the bolt |
| 72 | α | Parameter characterising the interaction in the axial direction between |
| 73 | | the bolt and the surrounding rock $\alpha = \sqrt{\frac{\beta_c \cdot P_{hole}}{EA}}$ |
| 74 | β | Parameter characterizing the interaction in the transverse direction |
| 75 | | between the bolt and the surrounding rock $\beta = \sqrt[4]{\frac{k \cdot \Phi_{hole}}{4 \cdot EJ}}$ |
| 76 | β_c | Ratio between the shear stresses, τ , that develop on the perimeter of the |
| 77 | | bolt and the relative axial displacements, v_r |
| 78 | δ_{max} | Maximum displacement component of the block in the axial direction of |
| 79 | | the bolt |
| 80 | φ | Friction angle on the natural discontinuity constituting the sliding surface |
| 81 | Φ_{bar} | Diameter of the steel bar |
| 82 | Φ_{hole} | Diameter of the hole (of the bolt) |

| | | |
|----|------------------|-------------------------------------------------------------------------|
| 83 | μ | Mean value of the distribution; |
| 84 | χ | Adimensional parameter for the evaluation of the stabilising forces |
| 85 | λ | Adimensional parameter for the evaluation of the stabilising forces |
| 86 | σ | Standard deviation of the distribution. |
| 87 | σ_{yield} | Steel yield stress |
| 88 | τ | Shear stress on the lateral surface of the bolt |
| 89 | τ_{lim} | Ultimate limit shear stress of the rock-bolt interface |
| 90 | ϑ | Inclination of the sliding surface with respect to the horizontal plane |
| 91 | | |

92 **Introduction**

93 During underground construction of different infrastructures, stability is expected,
94 therefore reinforcement is needed to keep the excavation stable (Pelizza et al., 2000).
95 A number of factors affect the underground stability in joint rock masses, e.g. high rock
96 stress, poor rock mechanical properties, excessive ground water pressure (Chen,
97 1994). Fully grouted passive bolts are widely used in the tunnel and underground
98 caverns as a stabilization intervention. Many studies have been carried out to describe
99 their behavior in rock masses considered to be homogeneous and continuous (Osgoui
100 and Oreste, 2007; Ranjbarbia et al., 2014; 2016; Oreste, 2013). Passive rock bolt
101 elements have a zero initial load and the mobilized stabilizing load increases with the
102 displacement of the potentially unstable rock block. Continuously mechanically
103 coupled (CMC) bolts rely on a curing agent (cementitious or resin grout; i.e. Spagnoli
104 et al., 2021) that fills the annulus between the element and the borehole wall (Bawden,
105 2011). Rock bolts are primarily stressed by tensile and shear loads, which are caused
106 by rock movements. The stress on the rock bolts depends on the type of rock failure
107 (crack fracture, folding, shear fracture etc.). The essential task of the rock bolt consists
108 in keeping the rock as stable as possible or to increase the shear resistance (Feder,
109 1980). Especially in tunnel construction, rock-bearing elements are in a statically
110 undetermined system with different rock stiffness values (Blümel, 1996). Ferrero
111 (1995) and Kilic et al. (2002) pointed out that the main factors affecting the shear and
112 bond strength of rock bolts are the rock bolts' materials, the geometry of the bolt (bolt
113 shape, diameter and length), type of binder, type of rock mass and fracture system.
114 Moosavi et al. (2002) proved that a stress decrease in poor-quality rock resulted in
115 completely ineffective bolt behavior. Therefore, any changes occurring at the bolt–
116 grout or grout–rock interface affect the bolt bond strength and bolt load capacity.

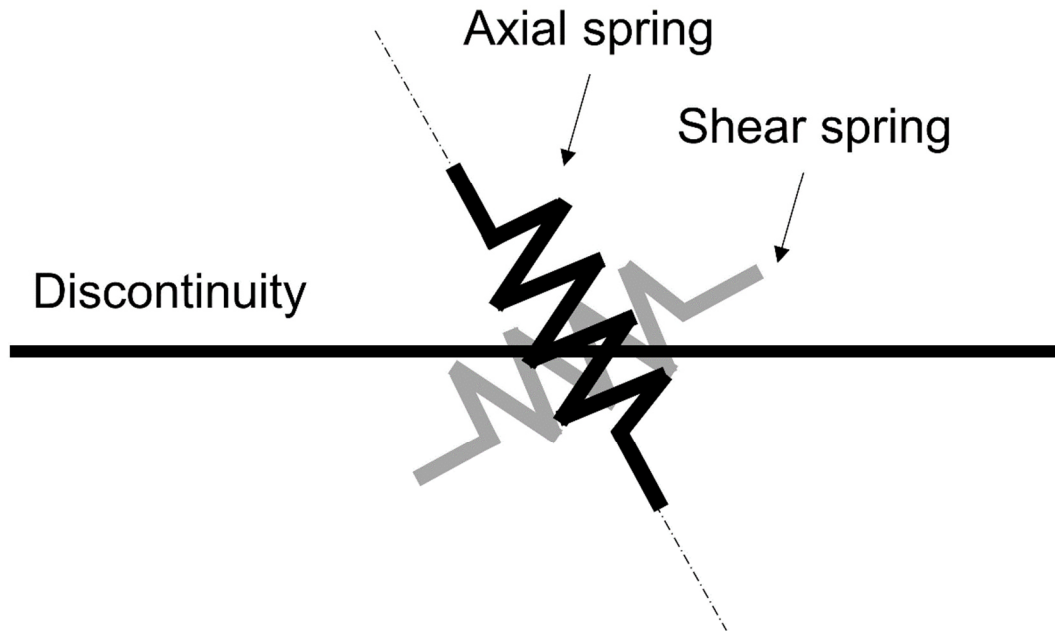
117 Recently Oreste et al. (2020) used the Block Reinforcement Procedure (BRP) (Oreste
 118 and Cravero, 2008; Oreste, 2009), to run a parametric analysis considering different
 119 diameter of the steel bar, thickness of the binder ring around the bar, length of the bolt
 120 in the unstable block, total length of the bolt, elastic modulus of the binder and
 121 inclination of the sliding surface of a rock block with respect to the horizontal plane.
 122 This model considers a bolt which crosses the potentially unstable block (with a length
 123 L_a) and reach the stable rock behind it, where it penetrates for a certain length (L_p),
 124 see Fig. 1.



125
 126 **Fig. 1 Schematic representation of the potentially unstable block of rock and the**
 127 **passive bolt crossing it (not to scale).**

128 The method allows to calculate the axial, N , and shear, T , forces, and the bending
 129 moments M developing along the bolt, as a linear function of the (very small)
 130 displacements of the block. Then the stabilizing forces, applied by the single bolt to
 131 the potentially unstable block, are evaluated. The rock-bolt interaction involves the
 132 presence of independent springs according to Winkler's approach, both in the

133 transverse and axial direction with respect to the bolt (Figure 2) (Oreste and Cravero,
134 2008).



135

136 **Fig. 2 Model for axial and shear springs at a discontinuity**

137 The parameters influencing the interaction are difficult to evaluate, because they
138 depend on the bending and axial rigidity of the bolts, on the stiffness of the grout
139 surrounding the bar, on the stiffness of the rock at the contour of the bolt. Furthermore,
140 laboratory tests are time-consuming to carry out.

141 In addition, the forces necessary to simulate the rock-bolt interaction during
142 movements, even very small, of the potentially unstable block of rock can be
143 considerable.

144 More recently, Oreste and Spagnoli (2020) have proposed simplified equations to
145 simulate the static contribution of fully grouted bolts on potentially unstable (by sliding)
146 rock blocks, in terms of axial and transverse force to the bolt. These equations are
147 reliable even if they are based on simplifying hypotheses: the errors are negligible,

148 considering the typical range of variability of the parameters influencing the rock-bolt
149 interaction. However, the problem of the reliable definition of the parameters
150 influencing the evaluation of the stabilizing forces of the potentially unstable block of
151 rock remains.

152 This work illustrates a new probabilistic approach able to manage the uncertainty on
153 various parameters that affect the behavior of bolts and to provide the probabilistic
154 distribution of the safety factor of the rock blocks for each different stabilization
155 intervention scheme. supposed. From the results obtained, it is possible to design the
156 stabilization work, for example by defining the diameter of the bolts required, based
157 on a greater knowledge of the effects of the uncertainty of the geotechnical parameters
158 on the degree of stability of the rock blocks. The same probabilistic approach used for
159 this specific stabilization problem can be adopted in other stability problems in the
160 geotechnical field.

161 After describing the proposed probabilistic procedure in the field of geotechnical
162 engineering and of rock mechanics, the stabilization mechanisms of passive fully
163 grouted bolts on rock blocks showing a potential planar slip are illustrated. Finally, the
164 application of the probabilistic approach to a specific real case will be illustrated.

165 The authors hope that the use of a probabilistic approach such as the one illustrated
166 in this work, which does not require the use of specific software or complex
167 procedures, will allow a more correct and responsible design of the engineering
168 interventions necessary in stability problems in geotechnical engineering.

169

170 **Proposed probabilistic approach in the evaluation of the safety factors in**
171 **geotechnical engineering**

172 The probabilistic analysis in geotechnical engineering evaluates the probability of a
173 certain event occurs considering certain data relating to the geotechnical properties of
174 the system (e.g. Griffiths and Fenton, 2009). Variability of ground properties
175 constitutes a major source of uncertainty when contending with geotechnical problems
176 (Franco et al., 2019). The adoption of probabilistic methods relating the uncertainty of
177 the different geotechnical properties on the final output has proven to be a valuable
178 approach (e.g. Tang et al., 1976; Ronold and Bysveen, 1992; Oreste, 2005; Spagnoli
179 et al., 2018; Spagnoli and Shimobe, 2020).

180 Several probabilistic techniques are used to account the uncertainty of the
181 geotechnical parameters. General probabilistic methods are used to quantify the
182 probability of occurrence of a single behavior (or property) for rocks and soils (e.g.
183 Schubert and Goricki, 2004; Oggeri and Oreste, 2012; Mollon et al., 2013; Oreste,
184 2015; Spagnoli et al., 2017). More specifically, Cherubini et al. (2004), Trivedi and
185 Zimmer (2005), Nelsen (2006), to name a few, modelled multivariate data based on
186 the copula theory in which a copula function instead of the correlation matrix is used
187 to represent the dependence relationship among random variables. For instance, Cao
188 and Wang (2014), Ching et al. (2016), Zhang et al. (2014), Contreras et al. (2018),
189 used a Bayesian method to characterize the spatial variability of soil (rock) properties,
190 quantify the model selection uncertainty and to compare the validity of the candidate
191 models. The point estimate method was used in geotechnical reliability analysis by
192 Schweiger et al. (2001) and Christian and Baecher (2002).

193 Monte Carlo technique, which involves generating a large number of random samples
194 from the input distributions and put into the transfer function, were investigated by
195 Oreste (2005), Sari et al. (2010), Aladejare and Akeju (2020).

196 In the absence of more detailed information on the probabilistic distributions of the
197 parameters considered uncertain in the calculation, the normal (Gaussian) distribution
198 is used, expressed by the following equation:

$$199 \quad f(x) = \frac{1}{\sigma \cdot \sqrt{2 \cdot \pi}} \cdot e^{-\frac{(x-\mu)^2}{2 \cdot \sigma^2}} \quad (1)$$

200 Where:

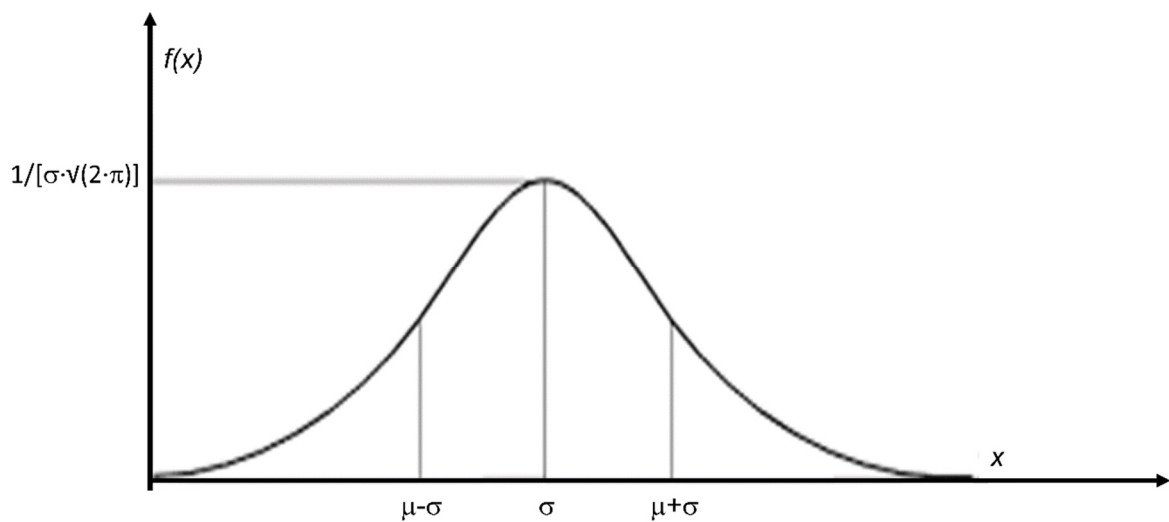
201 $f(x)$ is the is the probability density associated with the x value of the geotechnical or
202 geomechanical parameter considered;

203 μ is the mean value of the distribution;

204 σ is the standard deviation of the distribution.

205 The probabilistic distribution of Gauss is symmetrical and requires that 69.83% of
206 cases are included within the range $[\mu - \sigma]$ - $[\mu + \sigma]$, 95.45% of cases in the interval
207 $[\mu - 2\sigma]$ - $[\mu + 2\sigma]$ and 99.73% of cases in the interval $[\mu - 3\sigma]$ - $[\mu + 3\sigma]$ (Fig. 3).

208 More specifically, 95% of cases are included in the range $[\mu - 1.96\sigma]$ - $[\mu + 1.96\sigma]$ and
209 99% of the cases in the interval $[\mu - 2.58\sigma]$ - $[\mu + 2.58\sigma]$.



210
211 **Fig 3. Gauss probabilistic distribution trend used to represent the uncertainty**
212 **of the parameters in the geotechnical and geomechanical field.**

213 Therefore, starting from *in situ* or laboratory tests, it is possible to obtain samples of
214 measurements for each influential parameter (input data), in order to have an estimate
215 of the average values and standard deviations of the probabilistic distributions to be
216 adopted in the calculation. Alternatively, by identifying the variability interval of a
217 parameter x associated with a certain probability, p , that the real value falls within that
218 interval (for example 95% or 99%), it will be possible to determine the average value
219 μ and the standard deviation σ of the Gaussian distribution to be used in the
220 calculation:

$$221 \quad \mu = \frac{(x_{max} + x_{min})}{2} \quad (2)$$

$$222 \quad \sigma(p = 95 \%) = \frac{(x_{max} - x_{min})}{3.92} \quad (3)$$

$$223 \quad \sigma(p = 99 \%) = \frac{(x_{max} - x_{min})}{5.16} \quad (4)$$

224 Where x_{max} and x_{min} are respectively the minimum and maximum values of the
225 variability interval of x .

226 The procedure proposed in this article provides that all parameters considered
227 uncertain are described by a probabilistic distribution, while those considered certain
228 are described by a simple representative (deterministic) value.

229 Once the probabilistic distributions of the uncertain parameters ($x_1, x_2, \dots, x_i, \dots, x_n$,
230 where n is the total number of parameters considered uncertain) necessary for the
231 calculation are known, it is possible to proceed with the random extraction of the values
232 by adopting the Monte Carlo procedure.

233 If it can be assumed that these parameters are independent of each other, samples of
234 m values can be created for each parameter x_i , by ordering the values thus obtained.

235 At this point m data vectors are formed $[x_1, x_2, \dots, x_i, \dots, x_n]_{j=1 \text{ to } m}$ with all the
236 parameters present in the same position j of the extracted sequence, with j varying

237 from 1 to m . m is the number of random extractions that are performed for each of the
238 n uncertain parameters, using the probabilistic distributions of each parameter.

239 For example, if in the problem under examination there are 5 parameters considered
240 uncertain ($n = 5: x_1, x_2, x_3, x_4, x_5$) and 1000 extractions are adopted with the Monte
241 Carlo procedure ($m = 1000$), 1000 vectors can be obtained of input data, as shown
242 below:

$$243 [x_1; x_2; x_3; x_4; x_5]_{j=1}$$

$$244 [x_1; x_2; x_3; x_4; x_5]_{j=2}$$

245 ...

$$246 [x_1; x_2; x_3; x_4; x_5]_{j=999}$$

$$247 [x_1; x_2; x_3; x_4; x_5]_{j=1000}$$

248 After having built up a sample of values extracted from the probabilistic distribution of
249 each random variable, it is possible to proceed to the determination of the safety factor
250 of the problem under examination for each series of values obtained from the different
251 extracted samples. In this way it is possible to create a sample of values of the safety
252 factor which can then be statistically treated:

$$253 [x_1; x_2; x_3; x_4; x_5]_{j=1} \quad F_S (j=1)$$

$$254 [x_1; x_2; x_3; x_4; x_5]_{j=2} \quad F_S (j=2)$$

255 ...

$$256 [x_1; x_2; x_3; x_4; x_5]_{j=999} \quad F_S (j=999)$$

$$257 [x_1; x_2; x_3; x_4; x_5]_{j=1000} \quad F_S (j=1000)$$

258 The safety factor is calculated starting from the extracted values of the uncertain
259 parameters and from the representative values for those considered certain
260 (deterministic values, kept constant in the calculation). The next paragraph illustrates
261 how to evaluate the safety factor for the problem under examination: the stability of a

262 block of rock potentially unstable due to sliding on a planar surface, in the presence of
263 a stabilization intervention with fully grouted passive bolts.

264 The result of the procedure is a sample, with a number m of safety factor values, i.e.
265 $[(F_s)_1 ; (F_s)_2 ; \dots ; (F_s)_i ; \dots ; (F_s)_m]$.

266 In order to have a good representation of the uncertainties present, a value of m of the
267 order of a thousand values is generally required. If there is a degree of correlation
268 between 2 or more parameters, for these we proceed to the extraction of the values
269 considering the multivariate statistics, that is, for the Gauss distribution, in addition to
270 the average value and the standard deviation of each parameter, we also consider the
271 correlation coefficients between the pairs of related parameters.

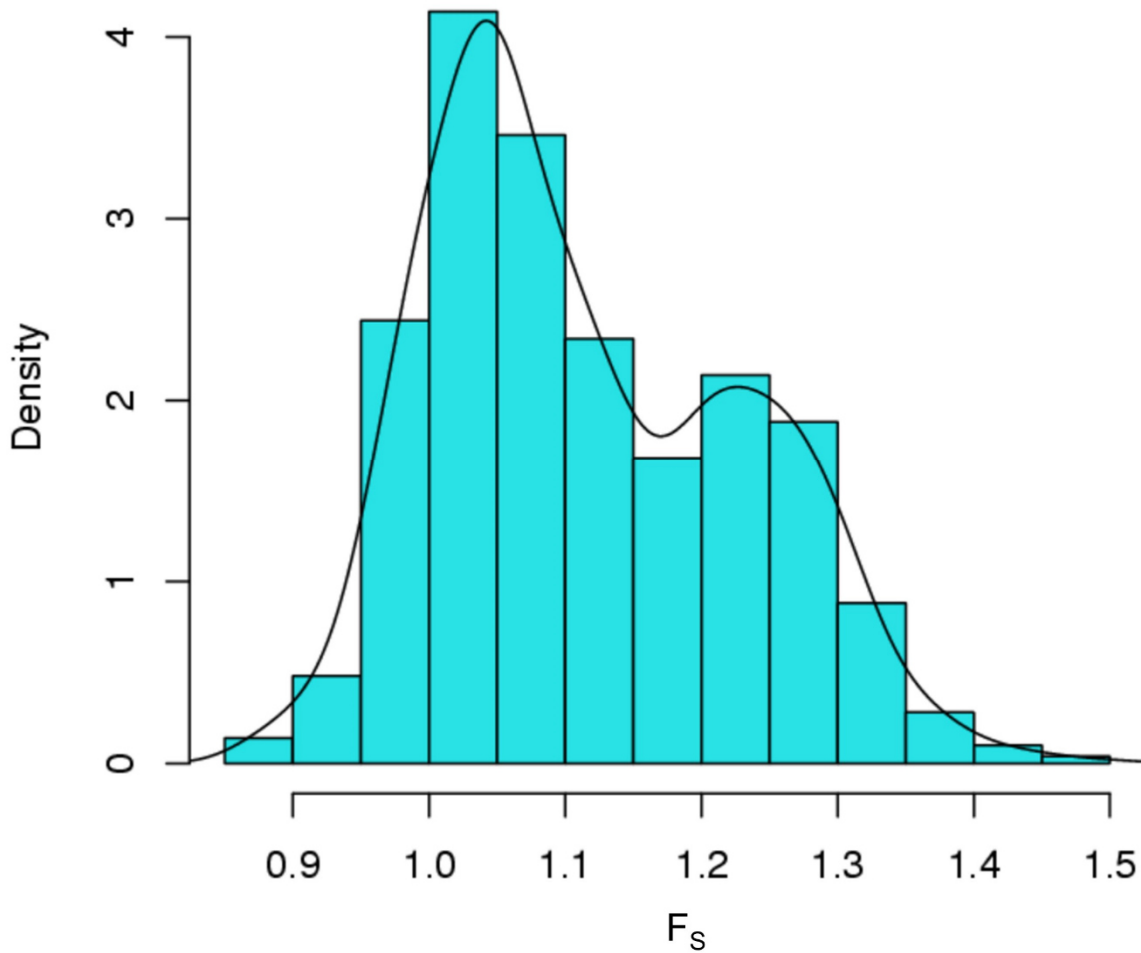
272 The analysis of the sample of the m values of the safety factor allows us to understand
273 the nature of its probabilistic distribution. Even if a Gaussian distribution is assumed
274 for each of the input data of the problem, the sample of the safety factor values in
275 general shows a probabilistic distribution different from the Gaussian one, which can
276 also have multimodal trends, such as the one shown in Figure 4.

277 It is important to check the sample of the safety factors obtained by analyzing the trend
278 of the histogram of the relative frequencies, in order to identify the theoretical
279 distribution that best represents the sample of the safety factors obtained from the
280 calculation.

281 Any confirmation of the theoretical distribution identified can then be made through the
282 Q-Q plot which compares the quantiles of the identified theoretical distribution with the
283 empirical quantiles on the sample data of the obtained safety factors.

284 The theoretical distribution that best represents the sample of safety factors allows
285 subsequently to have an indication of the probability that the safety factor is lower than
286 a certain predefined value $\overline{F_s}$. For example, it is very interesting to evaluate the

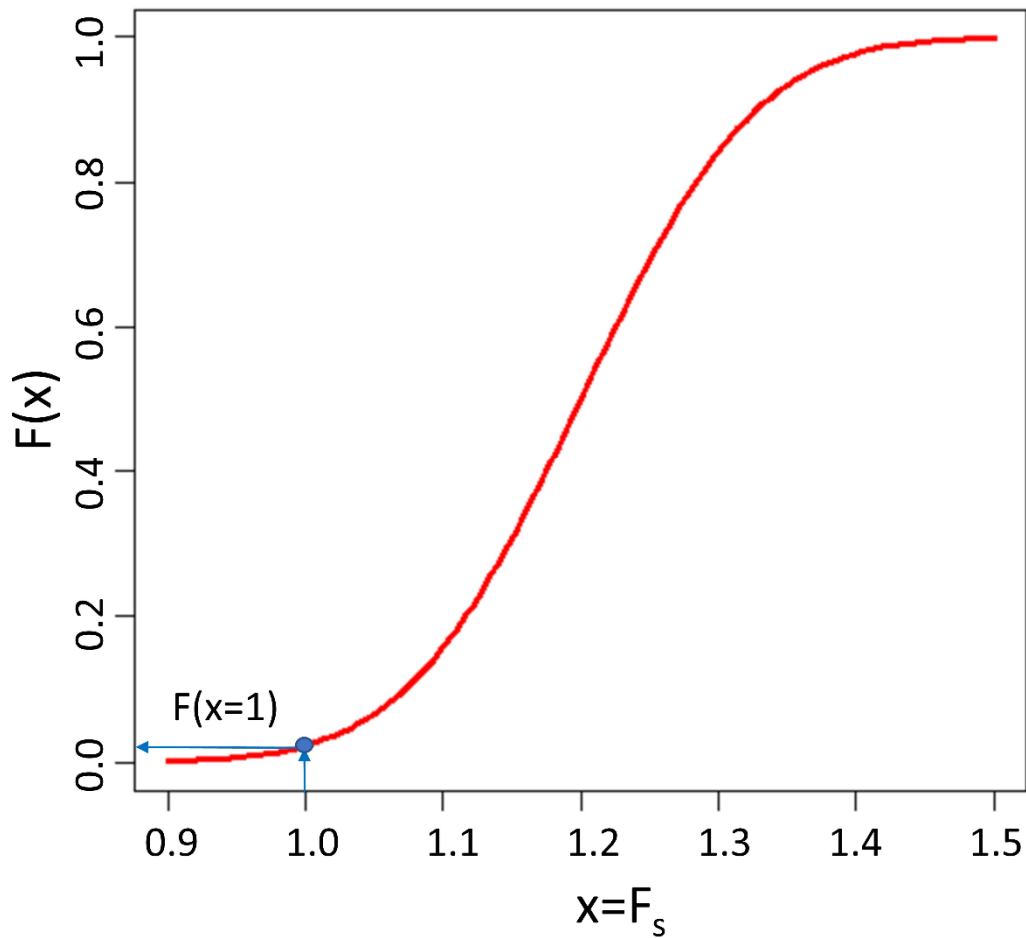
287 stability limit condition associated with a safety factor of 1 (i.e. $\overline{F_S} = 1$) and to determine
288 the probability that the safety factor is lower than this value ($F_S < \overline{F_S}$).
289 To do this, reference is made to the cumulative distribution of probabilities (Figure 5).



290

291 **Fig 4. General trend of the distribution of safety factors (F_S) obtained by**
292 **calculating the relative frequencies through the histogram.**

293



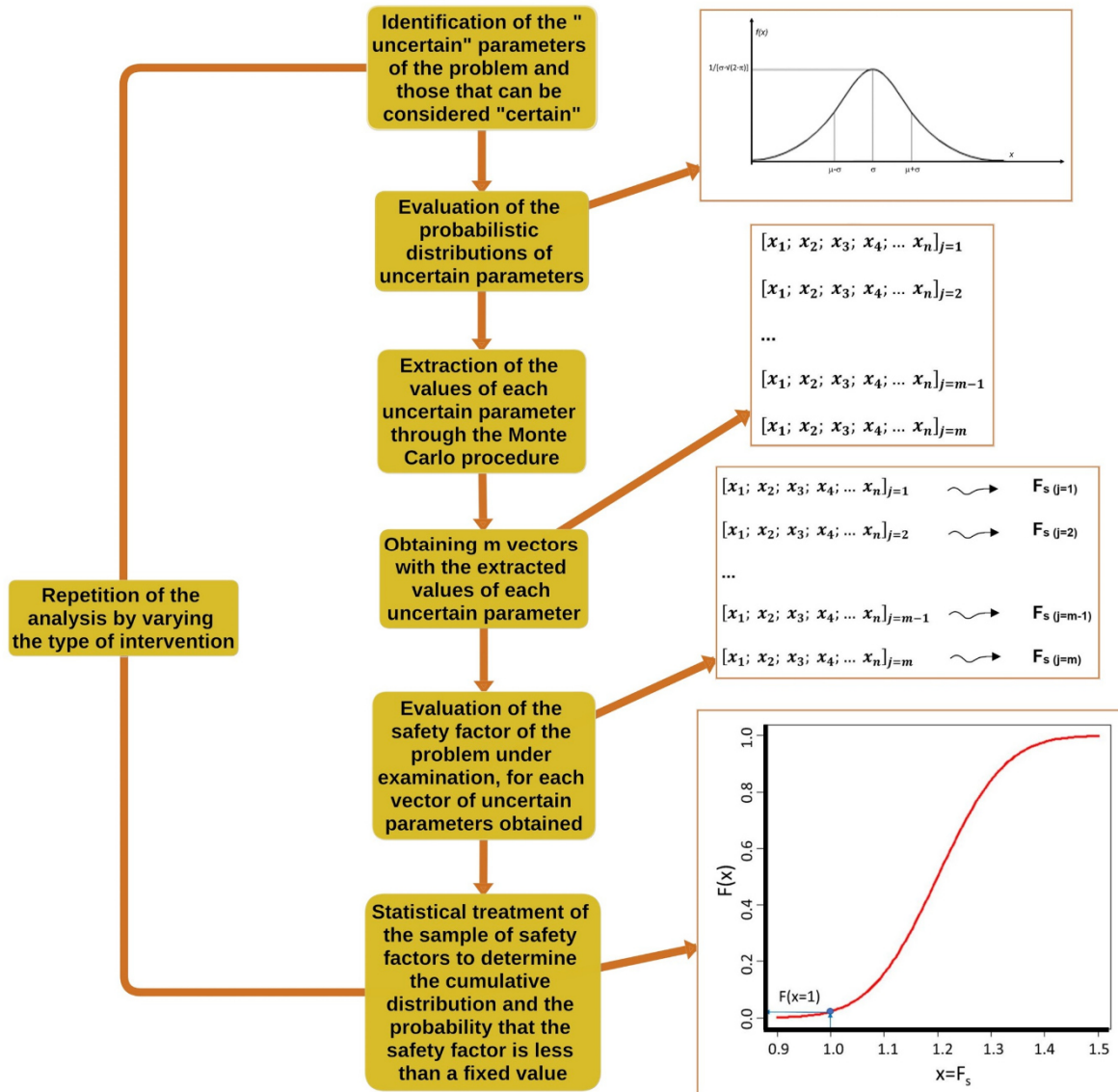
294

295 **Fig 5. Cumulative distribution of the probabilities (Gauss curve) of the safety**
 296 **factor, with indication of the probability $F(x = 1)$ that the safety factor is less**
 297 **than unity.**

298 This procedure can be carried out for the geotechnical problem under examination to
 299 ensure the stability of the soil or rock in the absence and in the presence of the
 300 supports and reinforcements to be designed.

301 A modern approach to the design of the interventions can therefore be conducted by
 302 checking whether the probability of instability is significantly reduced to very low and
 303 acceptable values in the presence of the supports and reinforcements of the soil or
 304 rock assumed in the project.

305 Figure 6 shows a summary flow chart of the proposed procedure in order to to perform
 306 the probabilistic analysis of the stability of a rock block in a simple and fast way in the
 307 presence of the planned stabilization interventions.



308
 309 **Fig 6. Flow chart of the procedure proposed for the evaluation of the stability**
 310 **conditions (through the evaluation of the safety factor) of a potentially unstable**
 311 **rock block, in the presence of stabilization interventions with fully grouted**
 312 **passive bolts.**

314 **Model description considering the stability of a two-dimensional block of rock**
 315 **with regard to sliding**

316 Fully grouted passive bolts develop internal forces linearly dependent on the
 317 displacements of the rock block that they must stabilize (Oreste and Cravero, 2008).
 318 The internal forces developed can be analyzed by referring to the interaction
 319 mechanism in the two directions perpendicular and parallel to the lateral interface of
 320 the bolt, in contact with the rock. There is a maximum displacement δ_{max} of the block
 321 for which the internal forces induce safety factors at breakage and extraction equal to
 322 the minimum ones considered admissible. The displacement δ_{max} is, therefore, to be
 323 considered as the maximum displacement of the block still compatible with the stability
 324 and efficiency of the bolt.

325 The shear T_0 and axial forces N_0 developing in the bolt at the point of intersection with
 326 an external surface of the block (which isolates the block from the stable rock behind)
 327 are also the stabilizing forces that the single bolt applies to the potentially unstable
 328 block. The maximum values of these forces that the bolt is able to offer to the block
 329 are obtained in correspondence with the displacement δ_{max} and are, therefore,
 330 indicated as $T_{0,\delta_{max}}$, and $N_{0,\delta_{max}}$ (Fig. 7).

331 Following a detailed parametric study within the typical variability ranges of the
 332 parameters influencing the bolt-rock interaction, it was possible to obtain the
 333 evaluation of the forces $T_{0,\delta_{max}}$, and $N_{0,\delta_{max}}$ that each single bolt potentially applies to
 334 the unstable block (Oreste and Spagnoli, 2020):

$$335 \quad T_{0,\delta_{max}} = \min \left(\frac{N_{yield}}{F_{s,adm,yield}} \cdot \frac{2}{\sqrt{\frac{\lambda^2 \cdot \chi^2}{\tan^2(\vartheta)} + \frac{64}{3}}}; \frac{N_{slip}}{F_{s,adm,slip}} \cdot \frac{2 \cdot \tan(\vartheta)}{\lambda \cdot \psi \cdot \alpha} \right) \quad (5)$$

$$336 \quad N_{0,\delta_{max}} = \min \left(\frac{N_{yield}}{F_{s,adm,yield}} \cdot \frac{1}{\sqrt{1 + \frac{64 \cdot \tan^2(\vartheta)}{\lambda^2 \cdot \chi^2}}}; \frac{N_{slip}}{F_{s,adm,slip}} \cdot \frac{\omega}{\alpha} \right) \quad (6)$$

346 τ_{lim} is ultimate limit shear stress of the interface rock-bolt;

347 N_{yield} is the force causing the bar failure under a tensile stress $N_{yield} = \sigma_{yield} \cdot A_{bar}$;

348 σ_{yield} is the yield stress of steel;

349 A_{bar} is the area of the section of the steel bar constituting the bolt $A_{bar} = \pi \cdot \frac{\Phi_{bar}^2}{4}$;

350 J_{bar} is the moment of inertia of the steel bar constituting the bolt, $J_{bar} = \pi \cdot \frac{\Phi_{bar}^4}{64}$

351 β is the parameter that characterizes the interaction in the transversal direction
352 between bolt and rock:

$$353 \quad \beta = \sqrt[4]{\frac{k \cdot \Phi_{hole}}{4 \cdot (EJ)_{bolt}}} \quad (9)$$

354 k is the ratio between the normal pressure, p , which is applied on the perimeter of the
355 bolt by the surrounding rock, and the transversal displacement, y , of the bolt;

356 α is a parameter characterizing the interaction in the axial direction between bolt and
357 rock as:

$$358 \quad \alpha = \sqrt{\frac{\beta_c \cdot \pi \cdot \Phi_{hole}}{(EA)_{bolt}}} \quad (10)$$

359 $(EA)_{bolt}$ is the axial stiffness of the bolt, evaluated as:

$$360 \quad (EA)_{bolt} = E_{st} \cdot \left(\frac{\pi}{4} \cdot \Phi_{bar}^2 \right) + E_{binder} \cdot \left[\frac{\pi}{4} \cdot (\Phi_{hole}^2 - \Phi_{bar}^2) \right] \quad (11)$$

361 $(EJ)_{bolt}$ is the bending stiffness of the bolt, evaluated on the basis of the following
362 equation:

$$363 \quad (EJ)_{bolt} = E_{st} \cdot \left(\frac{\pi}{64} \cdot \Phi_{bar}^4 \right) + E_{binder} \cdot \left[\frac{\pi}{64} (\Phi_{hole}^4 - \Phi_{bar}^4) \right] \quad (12)$$

364 Φ_{bar} is the bar diameter;

365 Φ_{hole} is the diameter of the hole where the bolt is inserted as $\Phi_{hole} = \Phi_{bar} + 2 \cdot t_{binder}$;

366 t_{binder} is the thickness of the binder annulus around the steel bar;

367 E_{st} is the steel elastic modulus;

368 E_{binder} is the elastic modulus of the binder surrounding the steel bar in the hole.

369 β_c is the ratio between the shear stresses developing on the perimeter of the bolt (on
370 the wall of the hole), τ , and the relative axial displacements, v_r . β_c depends in general
371 on the characteristics of the material surrounding the steel bar and on the elastic
372 modulus of the rock;

373 L_a and L_p are respectively the lengths of the bolt inside the potentially unstable rock
374 block (zone I) and in the stable rock (zone II); their sum is the total length of the bolt.

375 The normal (k) and tangential (β_c) stiffness parameters describe the bolt-rock
376 interaction and significantly affect the behavior of the bolt. Other fundamental
377 parameters are the values of the ultimate breaking stress of the bolt-rock interface
378 (τ_{lim}) and the strength of the steel (σ_{yield}).

379 ϑ is the angle that the sliding surface of the block forms with the horizontal plane. In
380 the typical case of horizontal bolts and perpendicular to the vertical rock wall, this angle
381 is also the angle that the sliding surface forms with the direction of the bolts.

382 A detailed parametric analysis, considering the typical variability of the parameters that
383 affect the bolt-rock interaction and, therefore, the behavior of the bolts, allowed to
384 evaluate the points where the bolt can fail.

385 Thanks to the evaluation of these points (Oreste and Spagnoli, 2020), it was possible
386 to identify simple summary equations of the maximum values of the two forces ($T_{0,\delta_{max}}$
387 and $N_{0,\delta_{max}}$) which still guarantee a certain safety margin with regard to the failure of
388 the bolt in the critical points identified by the parametric analysis. The parameters
389 falling within the equations are obtained by the *in situ* tests described in some detail in
390 the next paragraph.

391 The safety factor of the block, evaluated as the ratio between the resisting forces and
392 the unstable forces, is expressed by the following equation in the presence of the
393 stabilizing forces of the bolts (in the case of horizontal bolts):

$$F_s = \frac{c \cdot A + [(W - n \cdot T_{0,max}) \cdot \cos\vartheta + n \cdot N_{0,max} \cdot \sin\vartheta] \cdot \tan\varphi}{(W - n \cdot T_{0,max}) \cdot \sin\vartheta - n \cdot N_{0,max} \cdot \cos\vartheta} \quad (13)$$

395 Where:

396 c is the cohesion on the natural discontinuity which constitutes the sliding surface;

397 A is the area of the sliding surface of the block;

398 W is the weight of the potentially unstable rock block;

399 n is the number of fully grouted passive bolts present;

400 φ is the friction angle on the natural discontinuity constituting the sliding surface.

401

402 This equation reports at the numerator the stabilizing forces, which oppose the
 403 movement of the block, evaluated in the direction of sliding (i.e. the line of maximum
 404 slope on the sliding surface); the denominator includes the unstable forces, those that
 405 tend to move the block, also evaluated in the direction of sliding of the block.

406 This equation permits to proceed with the design of the bolts through the choice of the
 407 solution that allows to obtain the safety factor of the desired rock block. It is possible
 408 to proceed by trial and error, changing the geometric characteristics of the bolt
 409 (dimensions of the steel bar and of the entire bolt, length of the bolt) and the number
 410 of bolts, until the block is stabilized, with a safety margin considered acceptable.

411

412 **Application of the probabilistic approach to a real case**

413 There are several parameters influencing the safety factor of a rock block considering
 414 fully grouted passive bolts:

- 415 • cohesion and friction angle of the discontinuity representing the sliding surface;
- 416 • weight of the rock block, which is function of the volume and the specific weight
 417 of the rock;
- 418 • geometry of the bolts (of the steel bar and of the grout surrounding it);

- 419 • stiffness parameters of the bolt-rock interaction on the interface at the lateral
- 420 surface of the bolt;
- 421 • strength of the bolt-rock interface to bolt extraction;
- 422 • tensile strength of the steel constituting the bolt bar;
- 423 • elastic modulus of the steel and of the grout around the bar.

424 Several of these parameters are usually known only with some accuracy. In particular,
425 there are often large uncertainties on the stiffness parameters characterizing the
426 interaction between bolts and rock (k and β_c), on the strength of the bolt-rock interface
427 to bolt extraction (τ_{lim}), as well as on the cohesion (c) and friction angle (φ) of the
428 natural discontinuity representing the sliding surface. Specific laboratory tests are
429 carried out in order to evaluate these parameters, but from the tests it is possible to
430 obtain values that are often not very representative because the results can be
431 dispersive and the number of tests is generally limited.

432 To obtain the estimate of the cohesion and the angle of friction of the sliding surface,
433 shear tests are carried out on rock samples at the laboratory scale; to evaluate the
434 stiffness parameters of the bolt-rock interaction, specific load tests are prepared *in situ*
435 both in the axial and transverse direction of the bolt (Oreste and Spagnoli, 2020). To
436 determine the shear strength of the bolt-rock interface, we use the results pull-out tests
437 of a *in situ* test bolt with the application of a force in the axial direction.

438 The uncertainty about the evaluation of these parameters cannot be represented
439 simply by an average value of the results of *in situ* and laboratory tests. It is more
440 appropriate to consider a range of variability for uncertain parameters and associate it
441 to a certain probability that the real value falls within this range.

442 Such an approach was adopted to study the stabilization intervention of a block of
443 limestone potentially unstable due to flat sliding on a natural discontinuity with an

444 inclination of 35° with the horizontal plane (Oreste and Spagnoli, 2020). This
445 potentially unstable block, located on a municipal road in the northern part of Piedmont
446 (Italy), was analyzed to verify the need for a stabilization intervention with fully grouted
447 passive bolts and to design the intervention. Specific *in situ* and laboratory tests have
448 been developed.

449 The *in situ* tests on test bolts made it possible to obtain the stiffness coefficients of the
450 normal (k) and transverse (β_c) interaction of 8.90 ± 1.20 MPa/mm and 1.18 ± 0.38
451 MPa/mm respectively, with a confidence level of each variability interval greater than
452 99%.

453 The pull-out tests provided a stress limit of 2.08 ± 0.73 MPa. The shear tests
454 developed in the laboratory on samples including natural discontinuity, allowed to
455 determine the values of cohesion and friction angle of the sliding surface: $c = 8.0 \pm 2.3$
456 kPa and $\varphi = 23.0^\circ \pm 1.40^\circ$.

457 Assuming the mutual independence of the identified random variables and also
458 assuming a normal distribution (Gaussian probabilistic distribution), it is possible to
459 obtain the probabilistic distribution of each uncertain parameter and in particular the
460 standard deviation as well as the average value already known:

- 461 • cohesion c of the sliding surface: $\bar{x}_c=8.0$ kPa; $\sigma_c=0.89147$ kPa
- 462 • friction angle φ of the sliding surface: $\bar{x}_\varphi=23.0^\circ$; $\sigma_\varphi=0.54264^\circ$
- 463 • stiffness parameter β_c in the bolt-rock shear interaction: $\bar{x}_{\beta_c}=1.18$ MPa/mm;
464 $\sigma_{\beta_c}=0.14729$ MPa/mm
- 465 • stiffness parameter k in the normal bolt-rock interaction: $\bar{x}_k=8.90$ MPa/mm;
466 $\sigma_k=0.46512$ MPa/mm
- 467 • limit shear stress on the bolt-rock interface: $\bar{x}_{\tau lim}=2.08$ MPa; $\sigma_{\tau lim}=0.28295$ MPa.

468 The standard deviation was assumed to be $\frac{1}{5.16}$ of the width of the variability interval,
469 associating the latter with a confidence level of 99%.

470 The calculation of the safety factor F_S in the presence of some random variables can
471 be performed with the Monte Carlo method. After having built up a sample of values
472 extracted from the probabilistic distribution of each random variable, it is possible to
473 proceed to the determination of the safety factor for each series of values obtained
474 from the different extracted samples. In this way it is possible to create a sample of
475 values of the safety factor which can then be statistically treated.

476 If, for example, the number of the values of each sample obtained is m , it will be
477 possible to constitute m data series of the random variables, represented as follows:

478 [$(c)_1 ; (\varphi)_1 ; (\beta_c)_1 ; (k)_1 ; (\tau_{lim})_1$]

479 [$(c)_i ; (\varphi)_i ; (\beta_c)_i ; (k)_i ; (\tau_{lim})_i$]

480 [$(c)_m ; (\varphi)_m ; (\beta_c)_m ; (k)_m ; (\tau_{lim})_m$]

481

482 The result is a sample, with a number m , of safety factor values:

483 [$(F_S)_1 ; (F_S)_2 ; \dots ; (F_S)_i ; \dots ; (F_S)_m$]

484 The remaining parameters affecting the calculation of the safety factor were
485 considered known with an acceptable accuracy and remain constant during the
486 calculation:

- 487 • inclination ϑ of the sliding surface with respect to the horizontal plane: 35°;
- 488 • sliding surface area A : 10 m²;
- 489 • weight W of the block: 1080 kN;
- 490 • thickness of the grout ring t_{binder} around the steel bar: 0.01 m;
- 491 • length of the bolt inside the rock block L_a : 1.5 m;
- 492 • length of the bolt in the stable rock L_p : 2.5 m;

- 493 • elastic modulus of steel E_{st} : 210000 MPa;
- 494 • elastic modulus of the cementitious grout E_{binder} : 25000 MPa;
- 495 • yield strength of steel σ_{yield} : 400 MPa;
- 496 • safety factors required with regard to the failure of the bar $F_{s,adm,yield}$ and the
497 pull-out strength of the bolt-rock interface $F_{s,adm,slip}$: 1.25.

498 These parameters are considered for the evaluation of the safety factor of the block in
499 a deterministic way, with a value remaining constant in the calculation.

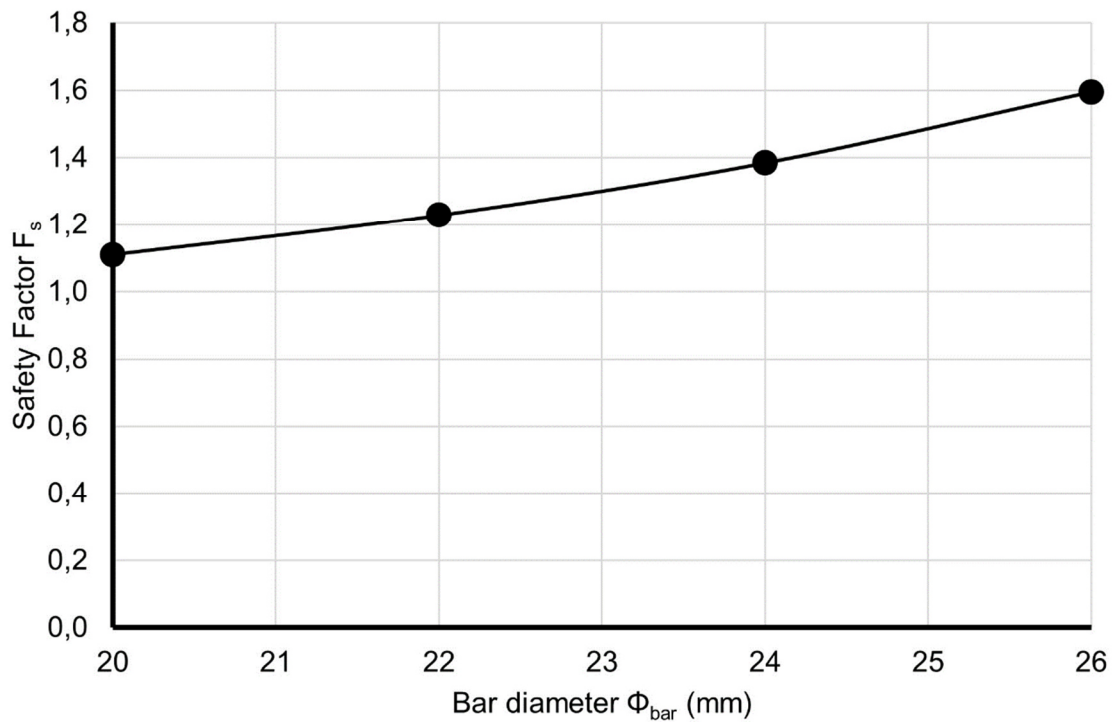
500 In natural conditions, without the effect of the stabilization intervention, the safety
501 factor was found to be 0.735 and, therefore, not sufficient to guarantee the stability of
502 the block.

503 To stabilize the rock block, it was decided to adopt two fully grouted passive bolts (n
504 = 2) with steel bars of ranging from diameter $\Phi_{bar} = 20$ mm to diameter $\Phi_{bar} = 26$ mm.

505 From the simple deterministic analysis considering the midpoint of the intervals of the
506 uncertain parameters it is possible to obtain the safety factor trend shown in Figure 7.

507 According to this approach, all the parameters present in the calculation take on a
508 constant (deterministic) value.

509 The traditional approach should involve setting the desired safety factor and obtaining
510 the smallest diameter of the bar able to achieve this value, using the graph in Fig. 8.



511

512 **Fig. 8. Trend of the safety factor of the block as the diameter of the steel bars**
 513 **change, based on a deterministic analysis of the safety factors, assuming the**
 514 **average value of the variability intervals of each as a representative value of the**
 515 **parameters considered uncertain.**

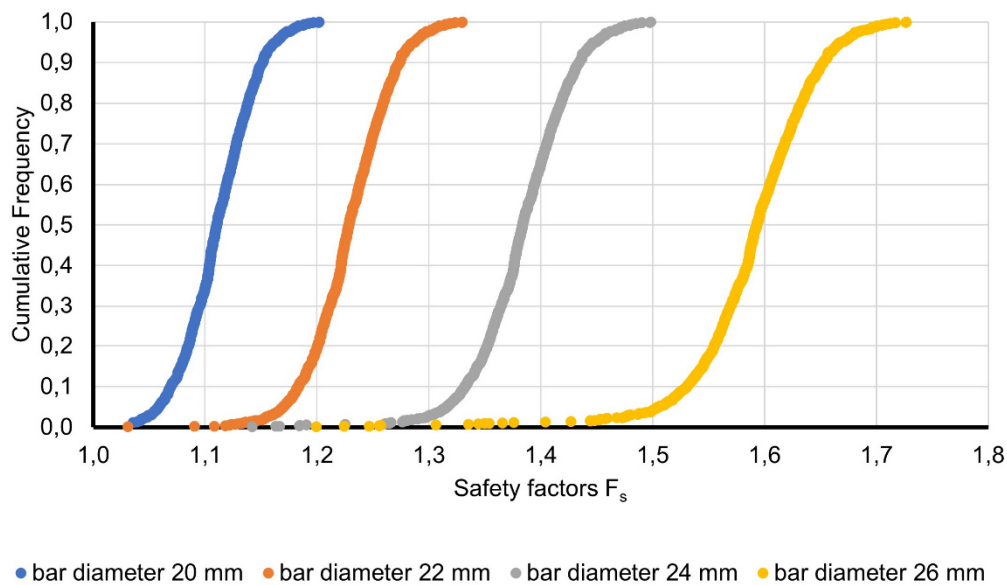
516 A subsequent and more in-depth probabilistic analysis using the Monte Carlo
 517 simulation allowed to obtain a different sample of the safety factors for each of the
 518 considered diameters. In total, therefore, 4 different samples, each consisting of
 519 thousand values of safety factors ($m = 1000$).

520 The Monte Carlo simulation is time consuming, even if for the proposed procedure the
 521 calculations proceeds rapidly, and the final solution is reached in a very limited time.

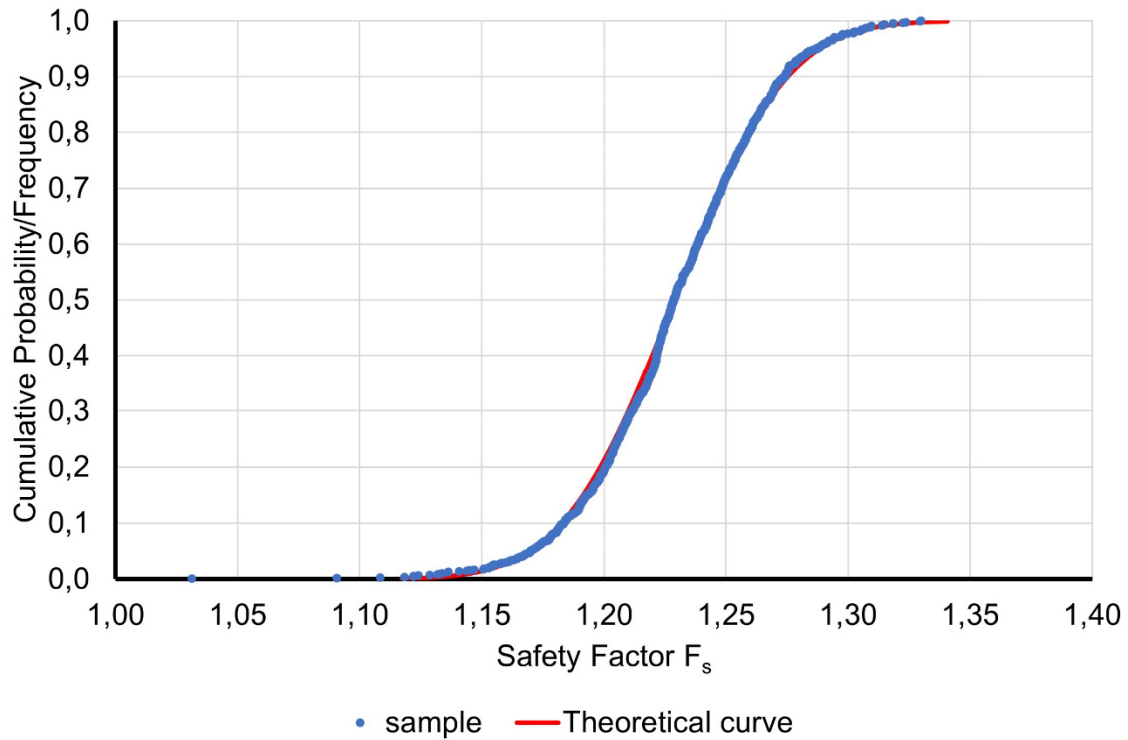
522 The m value to be adopted depends on the stabilization of the safety factor sample. It
 523 is necessary to continuously analyze the mean and standard deviation values of this
 524 sample until these values change significantly as the number of extractions increases
 525 and, therefore, as m increases.

526 Figure 9 shows the cumulative frequencies values for each of the 4 safety factor
527 samples obtained with the Monte Carlo simulation. After the verification of the
528 probabilistic distribution closest to the obtained samples, developed through traditional
529 analysis systems, it was possible to adopt the normal distribution of Gauss (Figures
530 10-12).

531 The comparison between the sample of safety factors and the theoretical distributions
532 available was made in relation to the cumulative frequencies, the Q-Q plot and the Box
533 Plot. Figures 10-12 show the comparisons adopting the normal distribution. Since the
534 comparison gave positive results, no further comparisons were made with other
535 different theoretical probabilistic distributions.



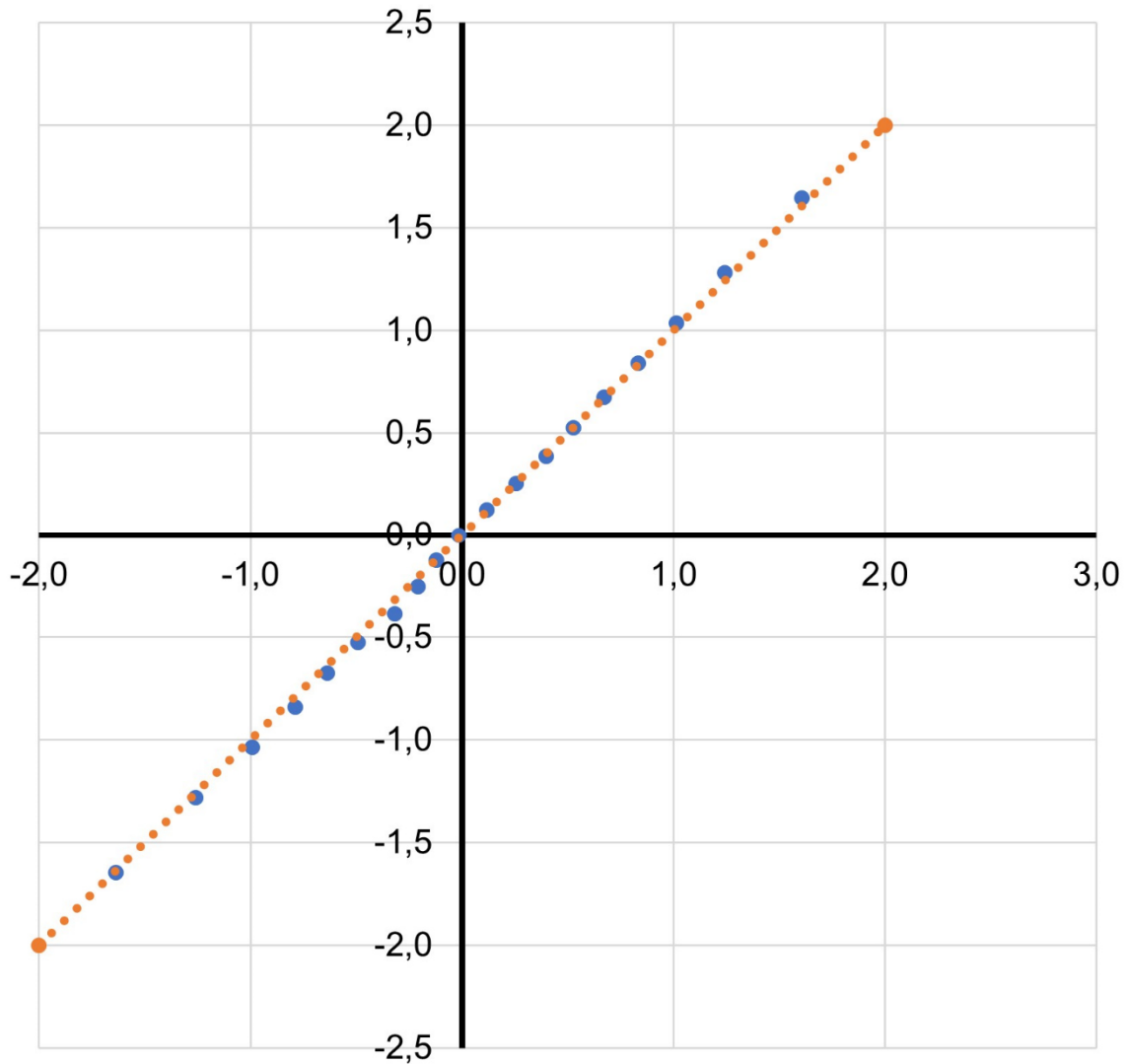
536
537 **Fig. 9. Trends of the cumulative frequencies of the safety factor samples**
538 **obtained from the calculation with the Monte Carlo procedure for the 4**
539 **diameters of the bars considered: 20 mm (blue), 22 mm (orange), 24 mm (grey)**
540 **and 26 mm (yellow).**



541

542 **Fig. 10. Verification of the distribution of safety factors for the case of a bar**
 543 **diameter of 22 mm ($\Phi_{bar} = 22$ mm) by comparing the cumulative sample**
 544 **frequencies and the theoretical curve of the cumulative Gaussian distribution.**

545



546

547 **Fig. 11. Verification of the distribution of safety factors for the case of a bar**
 548 **diameter of 22 mm ($\Phi_{bar} = 22$ mm) by examining the Q-Q plot relative to the**
 549 **comparison of the sample distribution with the theoretical curve of the**
 550 **cumulative distribution of Gauss .**

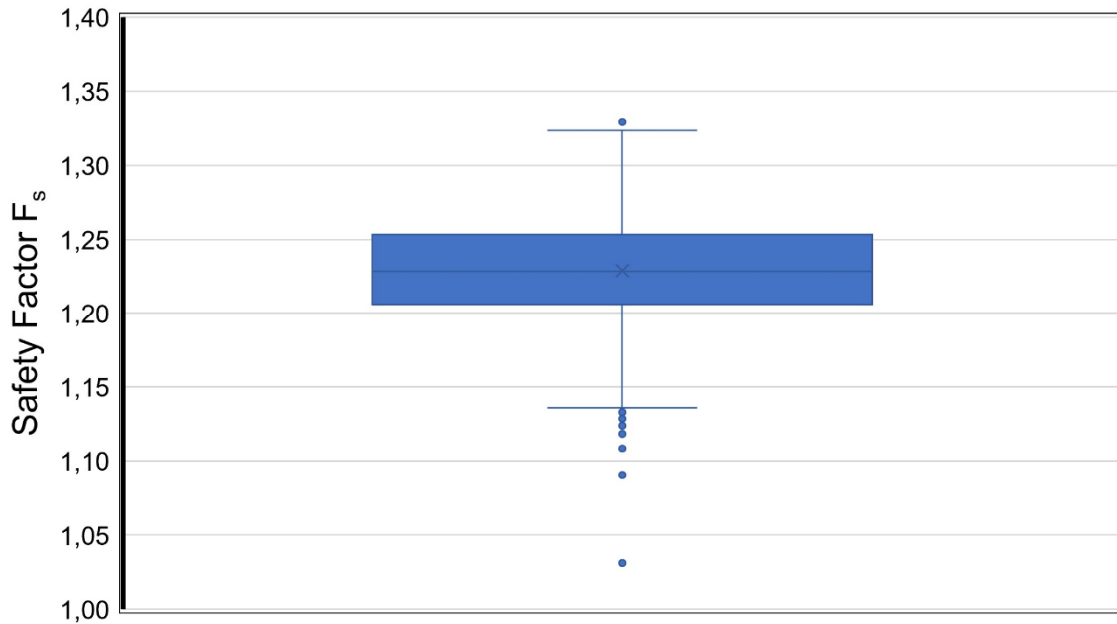
551

552

553

554

555



556

557 **Fig. 12. Verification of the characteristics of the sample of safety factors for the**
 558 **case of a bar diameter of 22 mm ($\Phi_{bar} = 22$ mm) by examining the Box Plot.**

559 After the verification of the samples allowed to consider the Gaussian normal
 560 probabilistic distribution as representative, it was possible to plot the cumulative
 561 probability curves for each diameter of the bar considered, referring to the mean
 562 values and standard deviations obtained for each sample:

563 $\Phi_{bar}=20$ mm: $\bar{x}_{FS}=1.111$; $\sigma_{FS}=0.032$

564 $\Phi_{bar}=22$ mm: $\bar{x}_{FS}=1.229$; $\sigma_{FS}=0.036$

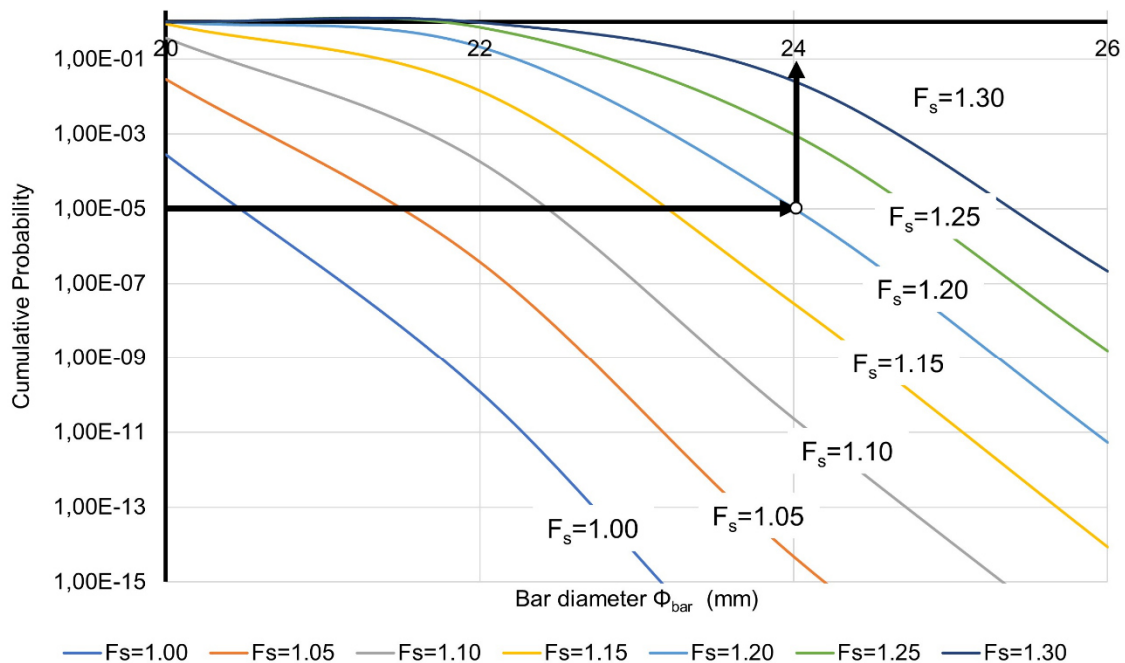
565 $\Phi_{bar}=24$ mm: $\bar{x}_{FS}=1.383$; $\sigma_{FS}=0.043$

566 $\Phi_{bar}=26$ mm: $\bar{x}_{FS}=1.590$; $\sigma_{FS}=0.057$

567 Thanks to the cumulative probability curves adopting the normal distribution, it is
 568 possible to evaluate, for each bar diameter, what is the probability that the safety factor
 569 is lower than a predetermined value. These probability values can be summarized in
 570 a graph as the one shown in Fig. 13. It is, therefore, possible to obtain, for example,

571 the indication to use a bar diameter equal to 24 mm to have a probability of only $1 \cdot 10^{-5}$
 572 ⁵ that the safety factor of the block is lower to 1.2.

573 It is possible therefore to obtain information of a probabilistic nature on the safety
 574 factors of a block of rock starting from the degree of uncertainty on the fundamental
 575 parameters of the problem under consideration, for each different diameter of the bar
 576 used. Such an approach, therefore, permits to consciously design the extent of the
 577 instability risks of a block of rock even in the presence of the stabilization intervention
 578 to be adopted, allowing for a modern and effective design of the interventions.



579
 580 **Fig. 13. Cumulative probability as the diameter of the bar varies for different**
 581 **values of the rock block safety factor. The graph permits to appropriately define**
 582 **the diameter of the bar necessary to allow having a predetermined probability**
 583 **that the safety factor is lower than a given value. In the example shown, it is**
 584 **possible to identify a bar diameter of 24 mm in order to limit the probability that**
 585 **the safety factor is less than 1.2 to 1 case in 100 thousand ($1 \cdot 10^{-5}$).**

586 The probability values were obtained with reference to a normal probabilistic
587 distribution, having the value of the mean and standard deviation equal to those of the
588 sample of safety factors obtained from the Monte Carlo simulation.

589 **Conclusions**

590 The stabilization of a block of rock on the walls of an underground cavity is usually
591 done through fully grouted passive bolts. The interaction mechanism between these
592 bolts and the surrounding rock is complex and is established only with a movement,
593 even if imperceptible, of the rock block.

594 Oreste and Cravero (2008) developed a calculation procedure for the evaluation of the
595 stabilization forces of passive bolts fully grouted on potentially unstable rock blocks.

596 More recently Oreste and Spagnoli (2020) identified some simplified formulas for the
597 definition of the stabilization forces of grouted passive bolts. However, the parameters
598 influencing the behavior of fully grouted passive bolts and leading to identify the extent
599 of the stabilization forces applied to potentially unstable blocks, are difficult to evaluate
600 and require specific laboratory tests or tests *in situ*. Such tests can be carried out only
601 in a limited number and often the results obtained are dispersive. Rather than precise
602 deterministic values, it is possible to estimate ranges of variability of the parameters
603 involved in the calculation.

604 A probabilistic approach is therefore necessary, which, starting from the uncertainties
605 of the parameters governing the bolt-rock interaction problem, leads to an assessment
606 of the possible variability of the safety factor of the rock block in the presence of
607 stabilization interventions.

608 In this article, a probabilistic approach has been proposed which is able to allow the
609 correct design of the passive fully grout bolts starting from the uncertainties on the
610 fundamental parameters of the bolt-rock interaction and on the resistance parameters

611 of the sliding surface of the block consisting of a natural discontinuity. This approach
612 is based on the Monte Carlo procedure and allows to obtain samples of the safety
613 factors for each different diameter of the steel bars of the bolts.

614 From the probabilistic analysis of these samples it was, therefore, possible to design
615 the steel bars considering the probability that the safety factor of the block with regard
616 to instability due to slipping is lower than a predetermined limit. In this way it is possible
617 to design a stabilization intervention by exploiting all the knowledge available on the
618 physical-mechanical phenomenon studied, including those relating to the uncertainty
619 of the fundamental parameters of the problem.

620 The proposed approach was applied with reference to a real case of a potentially
621 unstable rock block due to planar sliding on a natural discontinuity. The definition of
622 the diameter of the steel bars used for the stabilization intervention was obtained by
623 imposing that the block of rock may have a safety factor lower than 1.2 only for one
624 case out of one hundred thousand ($1 \cdot 10^{-5}$).

625 **Conflict of interests**

626 Authors declare they have no conflict of interest.

627 **References**

628 Aladejare AE, Akeju VO. Design and sensitivity analysis of rock slope using Monte
629 Carlo simulation. *Geotech Geol Eng* 2020; 38:573–585,
630 <https://doi.org/10.1007/s10706-019-01048-z>.

631 Bawden FW. Ground Control Using Cable and Rock Bolting. In: Darling P, editor. *SME
632 Mining Engineering Handbook*, Society for Mining, Metallurgy and Exploration Inc.,
633 Littleton; 2011. p. 616-617.

634 Blümel M. Untersuchungen zum Tragverhalten vollvermörtelter Felsbolzen im
635 druckhaften Gebirge. PhD thesis, Technical University, Graz, Austria; 1996.

636 Cao Z, Wang Y. Bayesian approach for probabilistic site characterization using cone
637 penetration tests. *J Geotech Geoenviron Eng* 2013; 139 (2):267–276.

638 Chen, D. Design of rock bolting systems for underground excavations. PhD thesis,
639 University of Wollongong, Australia; 1994.

640 Cherubini U, Luciano E, Vecchiato W. *Copula Methods in Finance*. Wiley, Chichester.
641 UK, 2004:

642 Ching J, Wu SS, Phoon KK. Statistical characterization of random field parameters
643 using frequentist and Bayesian approaches. *Can Geotech J* 2016, 53 (2). 285–298.

644 Christian J, Baecher GB. The point - estimate method with large numbers of variables.
645 *Int J Numer Anal Meth Geomech* 2002, 26(15):1515-1529.

646 Contreras, LF, Brown, ET, Ruest M. Bayesian data analysis to quantify the uncertainty
647 of intact rock strength. *J Rock Mech. Geotech* 2018, 10.11-31

648 Feder G. Zur Wirkungsweise und Gestaltung voll eingemörtelter Stabanker. *Tunnel*
649 1980; 2: 98–111.

650 Ferrero M. The shear strength of reinforced rock joints. *Int. J. Rock Mech. Min. Sci.*
651 *Geomech. Abstr* 1995; 32: 595-605.

652 Franco VH, Gitirana Jr, GFN, de Assis AP. Probabilistic assessment of tunneling-
653 induced building damage. *Comput Geotech* 2019; 113: 103097,
654 <https://doi.org/10.1016/j.compgeo.2019.103097>.

655 Griffiths, DV, Fenton, GA. Probabilistic settlement analysis by stochastic and random
656 finite-element methods. *J Geotech Geoenviron Eng* 2009; 135, 11: 1629-1637.

657 Kilic A, Yasar E, Celik, AG. Effect of grout properties on the pull-out load capacity of
658 fully grouted rock bolt. *Tunn Undergr Space Technol* 2002; 17: 355–362.

659 Mollon, G, Dias, D, Soubra, AH. Probabilistic analyses of tunneling-induced ground
660 movements. *Acta Geotech* 2013; 8:181–199, DOI 10.1007/s11440-012-0182-7.

661 Moosavi M, Bawden, WF, Hyett AJ. Mechanism of bond failure and load distribution
662 along fully grouted cable-bolts. *Mining Technology* 2002; 111:1-12.

663 Nelsen RB. *An Introduction to Copulas*, 2nd ed. Springer, New York; 2006.

664 Oggeri C, Oreste P. Tunnel static behavior assessed by a probabilistic approach to
665 the back-analysis. *Am J Appl Sci* 2012; 9(7): 1137-1144.

666 Oreste, P. A probabilistic design approach for tunnel supports. *Comp Geotech* 2005;
667 32:520–534.

668 Oreste PP. Face stabilisation of shallow tunnels using fibreglass dowels. *P I Civil Eng*
669 *Geotec* 2009; 162 (2):95–109, doi: 10.1680/geng.2009.162.2.95.

670 Oreste P. Face stabilization of deep tunnels using longitudinal fibreglass dowels. *Int J*
671 *Rock Mech Min Sci* 2013; 58:127-140.

672 Oreste, PP, Cravero, M. An analysis of the action of dowels on the stabilization of rock
673 blocks on underground excavation walls. *Rock Mech Rock Eng* 2008; 41(6): 835–868,
674 DOI 10.1007/s00603-008-0162-2.

675 Oreste P, Spagnoli G. A simplified mathematical approach for the evaluation of the
676 stabilizing forces applied by a passive cemented bolt to a sliding rock block. *Tunn*
677 *Undergr Space Technol* 2020; 103: 103459,
678 <https://doi.org/10.1016/j.tust.2020.103459>

679 Oreste P. Analysis of the tunnel-support Interaction through a probabilistic approach.
680 Am J Appl Sci 2015; 12(2): 121.129.

681 Oreste P, Spagnoli G, Buccoleri AG. A parametric analysis on the influence of the
682 binder characteristics on the behaviour of passive rock bolts with the Block
683 Reinforcement Procedure. Geotech Geol Eng 2020; 38:4159–4168
684 <https://doi.org/10.1007/s10706-020-01285-7>.

685 Osgoui RR, Oreste P. Convergence-control approach for rock tunnels reinforced by
686 grouted bolts, using the homogenization concept. Geotech Geol Eng 2007; 25(4):431-
687 440.

688 Pelizza S, Oreste P, Peila D, Oggeri C. Stability analysis of a large cavern in Italy for
689 quarrying exploitation of a pink marble. Tunn Undergr Space Technol 2000; 15(4):
690 421-435.

691 Ranjbarbia M, Fahimifar A, Oreste P. Practical method for the design of pretensioned
692 fully grouted rockbolts in tunnels. Int. J. Geomec 2016; 16(1): 04015012.

693 Ranjbarbia M, Fahimifar A, Oreste P. A simplified model to study the behavior of pre-
694 tensioned fully grouted bolts around tunnels and to analyze the more important
695 influencing parameters. J Min Sci 2014; 50(3): 533-548

696 Ronold KO, Bysveen S. Probabilistic stability analysis for deep-water foundations. J
697 Geotech Eng Div ASCE 1992; VI18(3): 394-405.

698 Sari M, Karpuz C, Ayday C. Estimating rock mass properties using Monte Carlo
699 simulation: Ankara andesites. Comput and Geosci 2010;36: 959–969.
700 [doi:10.1016/j.cageo.2010.02.001](https://doi.org/10.1016/j.cageo.2010.02.001).

701 Schubert W, Goricki A. Probabilistic assessment of rock mass behaviour as basis for
702 stability analyses of tunnels. In: Proc. Rock Mechanics Meeting, Stockholm, Sweden,
703 March 2004, 1-20, SvBeFo.

704 Schweiger HF, Thurner R, Pöttler R. Reliability analysis in geotechnics with
705 deterministic finite elements—theoretical concepts and practical application. Int J
706 Geomech 2001; 1(4):389-413.

707 Spagnoli G, Sridharan S, Oreste P, Di Matteo L. A probabilistic approach for the
708 assessment of the influence of the dielectric constant of pore fluids on the liquid limit
709 of smectite and kaolinite. Appl Clay Sci 2017; 145:37-43.
710 <https://doi.org/10.1016/j.clay.2017.05.009>.

711 Spagnoli G, Tsuha CHC, Oreste P, Mendez Solarte CM. A sensitivity analysis on the
712 parameters affecting large diameter helical pile installation torque, depth and
713 installation power for offshore applications. DFI Journal 2018; 12(3): 171-185.
714 <https://doi.org/10.1080/19375247.2019.1595996>.

715 Spagnoli G, Shimobe S. Statistical analysis of some correlations between
716 compression index and Atterberg limits. Env Earth Sci 2020; 79(24): 532.
717 [10.1007/s12665-020-09272-0](https://doi.org/10.1007/s12665-020-09272-0).

718 Spagnoli G, Carnelli, D, Wyink U, Herrmann C. Laboratory tests of fully grouted bolts
719 with a pumpable thixotropic resin. In: Barla M, Di Donna A, Sterpi D, editors.
720 Challenges and Innovations in Geomechanics. Springer International Publishing;
721 2021; Vol. 2: 1-8. https://doi.org/10.1007/978-3-030-64518-2_103 (in press).

722 Tang W, Yucemen M, Ang AS. Probability-based short term design of soil slopes. Can
723 Geotech J 1976; 13(3): 201–215.

724 Trivedi PK, Zimmer DM. Copula modeling: an introduction for practitioners. *Found.*
725 *Trends Financ* 2005; 1 (1): 1–111.

726 Zevgolis IE, Daffas ZA. System reliability assessment of soil nail walls. *Comp Geotech*
727 2018; 98, 232–242.

728 Zhang J, Huang HW, Juang CH, Su WW. Geotechnical reliability analysis with limited
729 data: Consideration of model selection uncertainty. *Eng Geol* 2014; 181:27–37.
730 <https://doi.org/10.1016/j.enggeo.2014.08.002>

731

732 **FIGURE CAPTION**

733 **Fig. 1 Schematic representation of the potentially unstable block of rock and the**
734 **passive bolt crossing it (not to scale).**

735 **Fig. 2 Model for axial and shear springs at a discontinuity**

736 **Fig 3. Gauss probabilistic distribution trend used to represent the uncertainty**
737 **of the parameters in the geotechnical and geomechanical field.**

738 **Fig 4. General trend of the distribution of safety factors (F_S) obtained by**
739 **calculating the relative frequencies through the histogram.**

740 **Fig 5. Cumulative distribution of the probabilities (Gauss curve) of the safety**
741 **factor, with indication of the probability $F(x = 1)$ that the safety factor is less**
742 **than unity.**

743 **Fig 6. Flow chart of the procedure proposed for the evaluation of the stability**
744 **conditions (through the evaluation of the safety factor) of a potentially unstable**
745 **rock block, in the presence of stabilization interventions with fully grouted**
746 **passive bolts.**

747 **Fig. 7 Sketch of the stabilizing forces applied by the fully grouted passive bolt**
748 **to the potentially unstable rock block on the walls of an underground cavity (not**
749 **to scale).**

750 **Fig. 8. Trend of the safety factor of the block as the diameter of the steel bars**
751 **change, based on a deterministic analysis of the safety factors, assuming the**
752 **average value of the variability intervals of each as a representative value of the**
753 **parameters considered uncertain.**

754 **Fig. 9. Trends of the cumulative frequencies of the safety factor samples**
755 **obtained from the calculation with the Monte Carlo procedure for the 4**

756 diameters of the bars considered: 20 mm (blue), 22 mm (orange), 24 mm (grey)
757 and 26 mm (yellow).

758 **Fig. 10. Verification of the distribution of safety factors for the case of a bar**
759 **diameter of 22 mm ($\Phi_{bar} = 22$ mm) by comparing the cumulative sample**
760 **frequencies and the theoretical curve of the cumulative Gaussian distribution.**

761 **Fig. 11. Verification of the distribution of safety factors for the case of a bar**
762 **diameter of 22 mm ($\Phi_{bar} = 22$ mm) by examining the Q-Q plot relative to the**
763 **comparison of the sample distribution with the theoretical curve of the**
764 **cumulative distribution of Gauss .**

765 **Fig. 12. Verification of the characteristics of the sample of safety factors for the**
766 **case of a bar diameter of 22 mm ($\Phi_{bar} = 22$ mm) by examining the Box Plot.**

767 **Fig. 13. Cumulative probability as the diameter of the bar varies for different**
768 **values of the rock block safety factor. The graph permits to appropriately define**
769 **the diameter of the bar necessary to allow having a predetermined probability**
770 **that the safety factor is lower than a given value. In the example shown, it is**
771 **possible to identify a bar diameter of 24 mm in order to limit the probability that**
772 **the safety factor is less than 1.2 to 1 case in 100 thousand ($1 \cdot 10^{-5}$).**

773